REPORT DOCUMENTATION PAGE

Form Approved
OMB NO. 0704-0188

1. AGENCY USE ONLY (Leave Blank)	2. REPORT DATE	3. REPORT TYPE AND DATES COVERED
	June 30, 2003	~~January 1, 2002 - June 30, 2003~~ 15 Jul 99 - 14 Jul 03

4. TITLE AND SUBTITLE
A Study of Atmospheric Seeing and It's Possible Improvement

5. FUNDING NUMBERS
DAAD19-99-1-0272

6. AUTHOR(S)
Charles H. Townes

7. PERFORMING ORGANIZATION NAME(S) AND ADDRESS(ES)
University of California
Physics Department
Berkeley, CA 94720

8. PERFORMING ORGANIZATION REPORT NUMBER

9. SPONSORING / MONITORING AGENCY NAME(S) AND ADDRESS(ES)
U. S. Army Research Office
P.O. Box 12211
Research Triangle Park, NC 27709-2211

10. SPONSORING / MONITORING AGENCY REPORT NUMBER
~~39874-EV~~
39874-EV-1

11. SUPPLEMENTARY NOTES
The views, opinions and/or findings contained in this report are those of the author(s) and should not be construed as an official Department of the Army position, policy or decision, unless so designated by other documentation.

12 a. DISTRIBUTION / AVAILABILITY STATEMENT
Approved for public release; distribution unlimited.

12 b. DISTRIBUTION CODE

13. ABSTRACT (Maximum 200 words)

Atmospheric density fluctuations which affect "seeing" have been studied to examine details of their characteristics and ways of at least partial compensation. Work involved two 60 ft erectable masts, each with five fast temperature sensors, and also measuring equipment set up on a pole at a height of 160 feet on the top of a rather narrow 160 ft. building. Wind speed measuring equipment was also installed. Extensive data has been taken as a function of height, horizontal separation, wind speed, and time of day. It has been found that the Kolmogorov-Taylor approximation has validity, but that there are important deviations from it. The power law of fluctuations as a function of frequency deviates somewhat from this KT model. The Taylor approximation for movement of fluctuations by wind is a reasonable approximation for modest distances but the time length of its validity is no longer than about 15 seconds. Major turbulences are shown to have similar vertical and horizontal sizes, and to vary in size approximately linearly with wind speed. Correction of approximately one half of the path length fluctuations of light passing through the earth's atmosphere appear to be possible from measurements monitoring fluctuations near the earth's surface.

14. SUBJECT TERMS			15. NUMBER OF PAGES
			16. PRICE CODE
17. SECURITY CLASSIFICATION OR REPORT UNCLASSIFIED	18. SECURITY CLASSIFICATION ON THIS PAGE UNCLASSIFIED	19. SECURITY CLASSIFICATION OF ABSTRACT UNCLASSIFIED	20. LIMITATION OF ABSTRACT UL

NSN 7540-01-280-5500

Standard Form 298 (Rev.2-89)
Prescribed by ANSI Std. 239-18
298-102

FINAL PROGRESS REPORT

Foreword

Although completion of work supported under this proposal has taken somewhat longer than expected, we believe it has achieved its goals and, at least for the location of Mt. Wilson where the studies were made, it has resulted in both a much clearer understanding of atmospheric seeing fluctuations and very much more detailed and quantitative information on seeing characteristics than was previously available. We are pleased with the results and they have now been rather completely described in scientific papers published or submitted for publication.

Statement of the Problem Studied

The goal of this proposal was "A Study of Atmospheric Seeing and Its Possible Improvement". Hence the nature of atmospheric fluctuations was measured and studied in detail in order to best understand the possibility of corrections or compensation for them, and in addition one paper was written which made and studied theoretically a particular new type of possible correction. Partly because a large fraction of seeing fluctuations occur near the ground, and partly because the equipment planned and used could practically measure fluctuations only within about 200 feet of ground level, the effects of low altitude seeing fluctuations were primarily studied. However, it was also demonstrated that much of the seeing problem is due to fluctuations at low altitudes.

Summary of the Most Important Results

Experimental work involved multiple simultaneous detections of atmospheric density fluctuations over a wide range of horizontal and vertical positions, at many wind speeds, and at many times during the day. This provided a rather more complete picture of atmospheric density fluctuations and their behavior than had been previously available.

Simultaneous measurements of turbulence at a number of points show that the Kolmogorov-Taylor model of atmospheric turbulence is a reasonable approximation, though measured deviations from it are of importance. The KT model predicts a power spectrum of fluctuations proportional to $\nu^{-5/3}$ for the higher frequencies, and a spectrum power independent of frequency at low frequencies due to an outer scale of turbulence. At very low altitudes, the power spectrum of temporal fluctuations in air density is found to vary somewhat more slowly than predicted. For example, averaging over all wind speeds the mean logarithmic slops of the power spectra are 1.73, 1.69, 1.59, 1.50, and 1.51 for altitudes of 9, 24, 39, 54, and 80 feet respectively as compared with the KT model values of 5/3, or 1.67.

The maximum size of major turbulence was found to vary substantially with wind speed, being approximately proportional to it for normal wind speeds. This striking dependence of turbulence size on wind speed has previously received little attention. At

wind speeds in the range of 2-8 m/s the major turbulence size is approximately 2.8sec · V, where V is the wind speed in meters per second. The size of major turbulence is thus in the range of 5-30 meters, depending on wind speed. This makes the frequency close to constant, i.e. approximately 0.1 Hz, at which the slope of the spectral power becomes less steep due to the outer scale of turbulence. The "outer scale" itself is comparable but slightly larger than this size of 5-30 meters, perhaps by a factor of 2. Dependence of turbulent size on wind speed has apparently not been previously noted.

The size of major turbulence was shown to be approximately the same in all directions, notable the same for horizontal and vertical directions. Such determinations have apparently not been made before, but they confirm the isotropy assumed by Kolmogorov.

The Taylor approximation of "frozen" turbulence clearly applies only over a limited time, since turbulent eddies develop and change over time. The time for major turbulence changes has been measured to be in the range of 10-15 seconds. Hence the distances over which the Taylor approximation applies are typically in the range of 10-100 meters, depending on wind speed. These are the distances for which a measurement of turbulence at one position can allow some useful prediction of turbulence downwind.

Near the ground, turbulence was found to decrease substantially in magnitude with increasing altitude. For altitudes of 9, 70, and 150 feet the relative magnitude of turbulence was found to be 1.0, 0.52, and 0.26, respectively.

By making adequate measurements near the ground, it appears practical to obtain useful correlations for perhaps one-half of the path-length fluctuations through the atmosphere and thus help stellar interferometry. Such measurements would appropriately be made up to an altitude of 100 feet or more, and preferable quite near the line of sight and at positions separated from the line of site in the same direction as the wind.

An alternative possibility for interferometry refinement, which uses light scattering to measure atmospheric densities, has also been shown to be possible. This involves use of a pulsed laser beam appropriately focused to provide a scattered signal independent of distance over an appreciable range. The total scattered signal then can provide a determination of total pathlength change over this distance due to density fluctuations.

Publications and Technical Reports Supported Under this Grant

(a) Papers published in peer-reviewed journals

"The Potential for Atmospheric Path Length Compensation in Stellar Interferometry", C. H. Townes, *Astrophysics Journal* **565**, 1376 (2002)

(b) Papers published in non-peer reviewed journals or in conference proceedings.

"Low Altitude Atmospheric Turbulence Characteristics at Mt. Wilson Observatory", N. Short, W. Fitelson, C. H. Townes, Proceedings for Optical Astronomy, W. A. Traub, etc., Proceedings of SPIE 4848, 802 (2003)

(c) Manuscripts submitted and to be published in a peer-reviewed journal, the *Astrophysics Journal*

"Low Altitude Atmospheric Turbulence Characteristics at Mt. Wilson Observatory", N. Short, W. Fitelson, C. H. Townes

Participating Scientific Personnel

Charles H. Townes, Professor of Physics
Nicholas Short, Physics Student
Walter Fitelson, Electrical Engineer
David Hale, Astronomer and Telescope Operator

Report of Inventions

No patentable inventions.

THE ASTROPHYSICAL JOURNAL, 565:1376–1380, 2002 February 1

THE POTENTIAL FOR ATMOSPHERIC PATH LENGTH COMPENSATION IN STELLAR INTERFEROMETRY

C. H. TOWNES
Department of Physics, 366 Le Conte Hall 7300, University of California, Berkeley, Berkeley, CA 94720-7300
Received 2001 August 17; accepted 2001 October 10

ABSTRACT

Adaptive optics provides a method for improving telescope imaging affected by atmospheric seeing distortions, but the differences in path length fluctuations through the atmosphere to two or more separate telescopes continues to limit the quality of stellar interferometry, and unfortunately is not ameliorated by adaptive optics. Some corrections to such fluctuations can be made by atmospheric density measurements near the ground, particularly since in some cases a substantial fraction of path length fluctuations occur in the atmosphere within 20–30 m of ground level. It is shown that more extensive corrections can be made by measurements of backscattered lidar radiation sent along the direction of the telescopes' observation. It is proposed that Rayleigh or Raman backscattering be used to measure changes in atmospheric density or index of refraction. Rayleigh scattering by molecules provides more intensity than does Raman and can allow path length corrections over distances of a few hundred meters to somewhat more than a kilometer with a fractional accuracy as good as 10^{-6} of the total atmospheric delay. Such measurements can substantially assist stellar interferometry. Details of how this might be done, and of likely errors and difficulties, are discussed quantitatively.

Subject headings: instrumentation: adaptive optics — instrumentation: interferometers — techniques: high angular resolution — techniques: interferometric

1. INTRODUCTION

The precision and sensitivity of spatial, or "stellar" interferometry done from the Earth's surface are usually limited by fluctuations in path lengths of stellar radiation through the atmosphere. Adaptive optics has recently been developed as a means of counteracting "seeing" fluctuations to improve images in a single telescope. For this, the wavefront of light arriving at a telescope is adjusted and made approximately planar over the telescope's aperture, thus producing an approximately diffraction limited image. However, this provides no correction for the "piston motions" or changes in relative path lengths to two separate telescopes which limit the quality of stellar interferometry. The relative fluctuations in atmospheric density along two or more parallel light paths from an object studied to the two or more separate telescopes used do not in themselves smear out images in a single telescope, but they rapidly change the relative phase of interfering beams and hence make difficult the measurements of maximum and minimum intensities in an interference pattern.

The atmospheric fluctuations in relative path lengths are usually more than one wavelength at optical or infrared wavelengths and make the interference between light collected by the two telescopes vary rapidly between maximum and minimum. As a result, interference fringes of the object to be observed may be badly smeared out. Experience with the magnitude and speed of fluctuations show wide variations, depending on atmospheric conditions, but indicate that path length corrections need to be made on a timescale as short as about 10^{-2} s for optical interference measurements, or about 0.2 s for interference of mid-IR (10 μm) wavelengths. If there is a nearby star of sufficient intensity to give strong interference patterns and make possible rapid corrections in the optical paths, it can be used to compensate atmospheric path length fluctuations. But unfortunately, often there is no star close enough and of adequate intensity for rapid corrections to be made. As a result, for a star which is not bright, good interference fringes from its radiation may not be obtainable.

For possible improvement of interferometry, changes in path lengths through the atmosphere may be determined by measuring the amount of scattered light from a laser beam directed by a telescope along the same path over which astronomical radiation is received. If water droplets or aerosols are not abundant, the scattering is proportional to atmospheric molecular density, and a sufficiently precise measure of its amount can determine fractional changes in index of refraction or path length. However, the amount of scattering, the precision with which measurements can be made over appropriately short times, and the accuracy with which the scattering is proportional to the index of refraction must all be examined.

Rayleigh, Raman, and Mie scattering of pulsed laser beams, or lidar, have already been extensively used over the last few decades to examine densities of various atmospheric components. Lidar has provided useful measurements of gravity waves and temperature structure in the high atmosphere, and of molecular and dust components (Pal et al. 1996; Ansmann, Riebesell, & Weitkamp 1990; Carswell et al. 1991; D'Altorio et al. 1993; Meriwether et al. 1994; Duck, Whiteway, & Carswell 1998; Whiteway & Carswell 1994; Whiteman, Melfi, & Ferrare 1992). Doppler lidar has also measured velocities in the high atmosphere (Rothermel et al. 1991; Gal-Chen, Xu, & Eberhard 1992). For a fixed atmospheric composition, the amount of Rayleigh scattering is proportional to the atmospheric density and hence can provide a measure of the index of refraction. Pulsed laser beams also allow determination of the location of the scattering and density measurement by timing of the scattered return signal. To determine densities of specific molecules, Raman scattering may be used. Mie scattering due to dust can be substantially greater than either Rayleigh or Raman scattering, but variation in dust density in the atmosphere both prevents its use for determination of atmo-

401

spheric density and can badly confuse measurements of density by Rayleigh scattering. Actual use of scattering for an adequately precise measurement of optical or infrared path lengths clearly requires careful examination of the variations expected, the precision required, and methods which might obtain such precision.

2. THE NATURE OF FLUCTUATIONS AND CORRECTIONS TO BE MADE

Density fluctuations in the atmosphere are usually approximated by the Kolmogorov model which, for two points separated by a distance r, predicts random relative fluctuations $\Delta\rho$ in density or Δn in index of refraction proportional to $r^{5/6}$. The Taylor approximation assumes a constant wind moving the atmosphere, which implies path length variations in time proportional to $t^{5/6}$, or a power spectrum proportional to $\nu^{-5/3}$, where ν is the frequency of fluctuation. Although the Kolmogorov-Taylor model is only an approximation, it provides a useful model and reasonable estimates of the relative magnitude and timescales for fluctuations important to various wavelengths and various beam separations. Very near the Earth's surface or for large distances r of separation, the model does not apply well.

A number of measurements of path length fluctuations through the atmosphere have been made; those associated with Berkeley's Infrared Spatial Interferometer (ISI) located at the Mount Wilson Observatory are examples. These show rough agreement with the power spectrum of fluctuations predicted by the Kolmogorov-Taylor approximation, but with a frequency variation of the power spectrum usually somewhat less that the predicted $\nu^{-5/3}$ (Bester et al. 1992). Amplitudes of fluctuations through the entire atmosphere are a few to a few tens of microns for reasonably good seeing. And under typical conditions at the Mount Wilson Observatory, about half of these fluctuations occur within 20–30 m height above the ground (Truehaft et al. 1995). The rapidity of path length fluctuations is highly variable depending on seeing conditions and wind speed. For most moderately good seeing conditions, the timescale for path length changes which are of the order $\lambda/20$ is as short as about 0.01 s for visible light ($\lambda = 500$ nm). For Kolmogorov-type fluctuations, this timescale varies as $\lambda^{6/5}$, so that at 10 μm wavelength it is approximately 1/3 s. Since it has been shown that one-half of the fluctuations occur within a few tens of meters of ground level, correction over a distance of only 20 m above ground level can be useful, and correction over the first 1000 m of path through the atmosphere may be very helpful. Hence, a goal for path length fluctuation correction might be to correct the 100–1000 m of lowest altitude in the path to a star with a precision of $\lambda/40$ for mid-IR wavelengths. More ambitious goals would be to correct such distances with a precision adequate for optical wavelengths, or over still greater distances. Since the index of refraction of air is approximately $1 + 2.7 \times 10^{-4}$, the air itself lengthens the "path length" over a distance of 1000 m by 27 cm. Hence, for a path length accuracy of $\lambda/40$, where $\lambda = 10$ μm, changes in average air density over the path should be measured to a fractional precision of one part in 10^6.

3. MEASUREMENT OF DENSITY FLUCTUATIONS BY RAYLEIGH SCATTERING

The cross section for Rayleigh backscattering by an individual air molecule is approximately $\sigma = 5.45(550/\lambda)^4 \times 10^{-28}$ cm^2 sr^{-1}, where λ is the wavelength in nanometers (Measures 1984). Hence, for light from an eximer XeCl laser with $\lambda = 308$ nm, an STP atmosphere backscatters a fraction 1.49×10^{-7} of the light per steradian per centimeter of air, or a total fraction of approximately 6.2×10^{-7} of the light per centimeter. The backscatter is enough to provide a substantial scattered signal from a powerful lidar. The wavelength 308 nm is absorbed by ozone in the high atmosphere but is transmitted at lower altitudes except for the atmospheric scattering. And the total atmospheric scattering by molecules is small enough not to weaken the laser beam by more than about 50% as it traverses an entire atmosphere of 8 km at NTP density. This assumes there is no fog or dust to produce additional scattering and attenuation. In fact, scattering by particles is commonly intense enough to confuse any measurements of molecular density by total Rayleigh scattering. However, for a first analysis aerosol scattering will be ignored, and avoidance of aerosol scattering will be discussed later. An NTP atmosphere will also be assumed for the present discussion. At altitudes substantially above sea level, which is typical of observatories, the lower air density decreases scattering but also makes the precision needed less, which gives a modest net advantage.

Consider use of a XeCl laser of 50 watts average power and 308 nm wavelength pointed directly along a telescope's line of sight and pulsed 100 times per second with pulses 10^{-8} s long. This is similar to the laser used by Duck (1999) for stratospheric measurements and similar to some lasers presently used for the artificial stars of adaptive optics. Backscattered light from the short pulse, 3 m in length, allows location of the scattering to a precision of a few meters if that information is needed. Each pulse contains 7.8×10^{17} photons and the backscatter per pulse from 3 m of STP air would be 3.5×10^{13} photons sr^{-1}. If backscattered light is collected by 65 inch diameter optics (such as that of the infrared spatial interferometer on Mount Wilson, cf. Hale et al. 2000) from a distance of 1000 m, the number of photons collected from each 3 m pulse is $3.5 \times 10^{13} \times \pi/4(1.65/1000)^2$, or 7.5×10^7. For measurement on a timescale of 0.3 s, which is adequately fast under reasonable good conditions for atmospheric fluctuations affecting wavelengths as long as 10 μm, 2.2×10^9 photons would be collected. This allows in principle a precision of one part in 4.7×10^4. Since the path length delay is 0.087 cm in 3 m of air, this gives an uncertainty of 1.9×10^{-6} cm or 1.9×10^{-3} wavelengths for 10 μm radiation. Path length positions closer to the telescope receiving the radiation provide larger solid angles and hence more photons, so the precision could be greater, but for evaluation of air density over varying distances the number of photons would need to be normalized to allow for changes in intensity as a function of distance. If distances are measured by timing pulses and normalization is done to allow for the stronger signals at closer distances, which would also produce smaller fractional errors, then the total error over 1000 m, summing the 3 m units, would be $2.0 \times 10^{-2}\lambda$, just slightly better than the goal of $\lambda/40$.

The above calculation of course assumes perfect detection, precise measurement of detector response, and accurate calibration to provide correct compensation for path length fluctuations. It also assumes no scattering due to dust (or a constant fractional amount) and an atmosphere

of constant composition (e.g., no variation in water content). High precision measurement of any atmospheric change is needed, but since the total fluctuations in path length which are rapid and need correction are normally only a few wavelengths, calibration of the overall scattering with an accuracy of only one part in a few hundred would be adequate and should not be difficult. Quantum efficiency of detection cannot be perfect but should be as large as 50%, and this imperfect efficiency could be compensated by a factor of 2 increase in laser power. Dark current in the detector is not likely to be a problem since the photon flux would be large. However, good quantum efficiency and elimination of any short-term fluctuations in responses of associated circuitry would be important. Any fluorescence produced in the atmosphere can be eliminated by detecting light only in a narrow wavelength band at the laser frequency. Most problematic is scattering by atmospheric dust, which will be discussed later. But atmospheric dust could also cause difficulties by attenuating the transmitted radiation, thus producing some inaccuracies in the measurement. Even the scattering by atmospheric molecules would reduce the radiation intensity received from a round trip of light to a distance of 1000 m by about 12%. This could require some compensation or might be a reason for using somewhat longer wavelengths which would have less scattering. However, it only represents an uncertainty in the calibration of any atmospheric change, and if such changes are no more than about 10 μm due to atmospheric fluctuations at the higher altitudes, the 12% error would not be very serious.

Another problem, probably a minor one, is the possibility of variation in atmospheric composition, particularly in water vapor content. Water molecules scatter light and contribute to the atmosphere's index of refraction just as do the molecules N_2 and O_2 of dry air. However, the ratio of scattering to index of refraction contributions are not the same for water and dry air. Rayleigh scattering is proportional to $(n-1)^2$, where n is the index of refraction of a gas at a standard molecular density; however, path length effects of the gas are proportional to $n-1$. Furthermore, $n-1$ is different for a given pressure of H_2O and one of dry air at the proposed laser wavelength of 308 nm, although essentially the same at 10 μm wavelength. If an atmosphere at standard constant density changes its H_2O content by 1 mm, and its density change is judged by the amount of Rayleigh scattering, it can be estimated that the index of refraction at 10 μm wavelength will be misjudged by approximately 8×10^{-8}. This would produce an error in assumed path length of 1 μm, or $\lambda/10$ for $\lambda = 10$ μm, in a distance of 12.5 m. It is not clear how rapidly humidity typically varies over short distances in a normal atmosphere, but changes over short distances, such as those between telescopes, which are as large as 1 mm of pressure seems unlikely under reasonably good conditions.

A technical problem which has so far been ignored is appropriate focussing of backscattered light at distances varying from 1000 m to perhaps only 10 m from the photon-collecting surface of the telescope. But it is in fact convenient and of some advantage to make no such variation in focus because a focus only at the longest distance to be used can ensure that the total backscatter received by a suitable detector is constant per unit path length, independent of distance to the scattering location. An aperture may, for example, be in front of the detector which admits only light focused by the receiving telescope within a solid angle subtended by the transmitted parallel beam at the maximum distance of 1000 m. Since the solid angle received is constant, this reduces the fraction of the transmitted beam observed by the factor $(D/1000)^2$, where D, the distance to the scattered light, is smaller than 1000 m. Hence, the amount of light received per unit distance is constant out to 1000 m, or at whatever distance the entire beam diameter is received. The ISI telescope's focal length of 5 m and diameter of 1.65 m requires an aperture at the detector of 0.82 cm to receive backscatter from the entire beam diameter at 1000 m. This arrangement obviates any need for determining distances to the scattered radiation, or for renormalization of intensities received. It does, however, weaken signals from distances shorter than 1000 m and make probable errors per unit length constant over the path rather than improving at the shorter distances. As shown above, the theoretically allowed precision in determining path length due to 3 m of air at 1000 m, using the laser power and collecting areas given as an example, is 2.0×10^{-3} wavelengths at 10 μm. For the entire 1000 m in distance it would then be $(1000/3)^{1/2} \times 2.0 \times 10^{-3}$, or 3.7×10^{-2} wavelengths. This is only a factor of 1.5 poorer than the goal suggested, and increased laser power could improve it. Although such an arrangement does not in principle provide quite as much precision as would the full use of all scattered light at distances shorter than 1000 m which was discussed earlier, it is substantially simpler and probably would in actual practice allow close to the same precision. Furthermore, since timing of returning pulses would not be necessary, it would be natural to use all backscattered light received by the detector for path length corrections, and this would include some light scattered from distances larger than 1000 m, providing partial corrections for somewhat larger distances.

Another technical problem which would need to be dealt with is the effect of the proposed intense laser pulses on detection of stellar radiation for the interference process. Since the laser wavelength would be different from that where interference is being measured (in the example given 308 nm vs. 10 μm), the interferometer detectors can be isolated by dichroic beam splitters and filters. If reasonably fast detectors are used, they might also be isolated from pulsed laser light by pulsed control of bias voltages without appreciable loss of signal integration time.

The example discussed here involves path length corrections adequate for substantial improvement of interferometry in the mid IR region. For optical wavelengths some corrections could be made by similar techniques, but they would be more limited. The shorter wavelengths would require an order of magnitude more precision in path length measurement, and the timescale of fluctuations would require measurements on a timescale at least an order of magnitude shorter. However, measurements could be made to eliminate fluctuations closer to the ground than 1000 m or to give approximate corrections over larger distances. Such approximate corrections may simplify the mechanical tracking of path length changes of the type which is normally done for stellar interferometry at optical wavelengths.

The most substantial uncertainty in the path length measurement procedure outlined above is the likely presence of dust or other aerosols in the line of sight which could backscatter more light than the molecules. If the aerosol concentration were constant throughout the path being measured,

this would not cause a problem, because any fluctuations would still represent fluctuations in air density. However, variations in aerosol concentration must be expected. And in many cases at low altitudes, aerosol scattering is substantially larger than Rayleigh scattering from molecules and is likely to make useful precision in density fluctuations unobtainable. The use of short wavelengths tends to minimize the ratio of Mie to Rayleigh scattering, and there may be some astronomical observing sites at relatively high altitudes where aerosol concentration would not be a severe problem for the type of measurement outlined above. However, measurements of a dry atmosphere at a kilometer altitude and higher have shown aerosols, presumably man-made, abundant enough to produce Mie scattering within an order of magnitude as large as that of the air molecules (Müller et al. 1998). And fluctuations in relative aerosol density would cause problems with measurement of air density variations. Aerosol fluctuations would clearly need to be examined carefully at any particular site if measurements of the type discussed above are to be used.

4. MEASUREMENT OF DENSITY FLUCTUATIONS BY RAMAN SCATTERING

An alternative to Rayleigh scattering as a measure of density fluctuations is Raman scattering, since a specific Raman frequency identifies a particular molecular component and cannot be produced by Mie scattering from aerosols. Its possible use will hence be discussed. The Raman backscatter cross section from a nitrogen molecule for incident light of the wavelength 308 nm considered above is approximately 4×10^{-30} cm^2 sr^{-1}, making N_2 Raman scattering in the atmosphere roughly 1000 times smaller than the total Rayleigh scattering. This would decrease precision by a factor of about 30 for the same laser intensity and collection techniques discussed above. Such a decrease, with a resulting precision in measurement of path length changes of only $\frac{3}{4}\lambda$ for $\lambda = 10$ μm, would not by itself provide good interferometric measurements, so other modifications in parameters need to be considered.

The general arrangement discussed above for collection of photons of the same number per unit path length regardless of the distance appears very convenient and does not lose precision by any large amount, so it will be assumed to always apply while other parameters are changed. For this case, the number of photons which must be collected is proportional to the square of the total distance L over which measurements are to be made, since the fractional precision must be proportional to $1/L$ and the randomness of scattering produces fluctuations in numbers of photons proportional to the square root of the number. The number collected per united length is proportional to $1/L^2$, where L is the maximum distance of the measurement. And the total number of photons collected is

$$n = \frac{a\sigma PD^2 t}{L},$$

where a is a proportionality constant, σ is the scattering cross section per molecule, P is the laser power, L is the total path length over which collection occurs, D is the diameter of the telescope aperture receiving the photons, and t is the time over which photons are collected in order to measure path length fluctuations.

Since the number of photons which must be collected to provide a given precision is proportional to L^2, to use Raman scattering from N_2 molecules over a distance L_1 rather than Rayleigh scattering from all molecules over a distance L requires

$$\frac{n_1}{L_1^2} = \frac{n}{L^2},$$

or

$$\frac{\sigma_1 P_1 D^2 t_1}{L_1^3} = \frac{\sigma PD^2 t}{L^3},$$

where the quantities with subscript 1 apply to the Raman scattering case and the others to Rayleigh scattering. For the same power, telescope diameter, and time, $L_1^3 = L^3\sigma_1/\sigma$, or $L_1 = (1/10)L$ since $\sigma_1 \approx 10^{-3}\sigma$.

If path length fluctuations can be measured only over the first 100 m of path by Raman scattering instead of 1000 m, is this large enough to be useful? As noted above, Truehaft et al. (1995) have shown that under normal observing conditions on Mount Wilson, approximately 50% of the path length fluctuations occur in the first 20–30 m along the line of sight of an observing telescope. While conditions can be quite variable, and it is not clear how much of the total path length fluctuations occur in the next 75 m beyond the first 25, it appears that path length corrections over a distance in the atmosphere even as short as 100 m, which appears practical with Raman scattering, may be quite useful.

To what extent can Raman scattering be extended beyond 100 m? Since from the above expressions,

$$L_1 = L\left(\frac{\sigma_1 P_1 D_1^2 t_1}{\sigma PD^2 t}\right)^{1/3},$$

one can consider increasing power, perhaps by a factor as large as 10, and using a large subsidiary "light bucket" collector with diameter D_1 of 5 m instead of the value 1.65 m for D. This would increase L_1 to 450 m, which should provide useful path length corrections.

Although the ratio of N_2 to O_2 in the atmosphere probably does not vary appreciably over a short time, the amount of H_2O may vary, which means that measurement of N_2 densities alone may not allow a determination of variations in optical path lengths to sufficient accuracy. The probability of short-term fluctuations in water vapor content is not well known and would need to be measured in order to determine how seriously this affects path lengths. If in fact it does change path lengths in a troublesome way, the water vapor density in the optical path would need to be measured as well as that of N_2. This could be done by Raman scattering of the laser radiation by H_2O. The Raman scattering cross section of H_2O is approximately 2×10^{-29} cm^2 sr^{-1} at a wavelength of 308 nm, which is 5 times larger than that of N_2. Detection of the separate Raman spectra of N_2 and H_2O would be needed, but would not add much complexity to a system designed to isolate the Raman spectrum of N_2 alone.

5. RESOLUTION OF AEROSOL FROM MOLECULAR SCATTERING—PROBABLY THE OPTIMAL APPROACH

If aerosol scattering is large enough to interfere with accurate measurement of atmospheric density by Rayleigh backscattering, as is probably commonly the case, it may be spectrally separated from molecular scattering. This is an

alternative to the use of Raman scattering, which will provide substantially more scattered intensity and precision than the Raman scattering possibility.

Backscattered light from air molecules will be Doppler shifted due to kinetic motion of the molecules and spread out over a fractional spectral range of approximately

$$\frac{2}{c}\sqrt{\frac{2kT}{m}},$$

where m is the molecular mass, T is the air temperature, and k and c are the Boltzmann constant and velocity of light, respectively. For a wavelength of 308 nm, this corresponds to a spread of ± 0.09 cm^{-1} for N_2 molecules at a temperature of approximately 300 K. The frequency spread due to thermal motions of aerosols or the wind velocity would be no larger than about 0.001 cm^{-1}. Hence, high spectral resolution which eliminates the Mie scattering by aerosols could allow approximately 90% of the Rayleigh scattering by molecules to be used for air density measurements. This would provide more photons by a factor of about 1000 than would the use of Raman scattering. It could thus provide more precision in density measurements over large distances than the Raman scattering technique discussed above, though it could not make separate measurements of both N_2 and H_2O as could the use of Raman scattering.

For the spectral resolution needed to separate molecular from aerosol scattering, the laser used must have a spectrum as narrow as a few hundredths of a wavenumber. Pulses of 10^{-8} s would imply widths of about 0.001 cm^{-1} and hence would not produce a troublesomely wide spectrum. Spectral separation of aerosol and of molecular scattering has already been demonstrated. For example, Piironen & Eloranta (1994) have used a tunable Nd:Yg laser and absorption of its radiation by iodine vapor to remove the aerosol backscatter. Precision of these earlier experiments was not enough to measure atmospheric densities adequately for stellar interferometry, but the techniques used can be applied for this purpose.

Removal of the narrow spectrum of light due to Mie scattering by aerosols should allow the precision and the measurement of path lengths to be essentially similar to those discussed in the earlier section on Rayleigh scattering. It would not allow separate corrections for water vapor content as would measurement of Raman scattering, but path length problems due to rapid variation in water vapor density would probably not be large. Hence, this approach appears to be the more promising way of obtaining substantial path length fluctuation measurement and correction.

6. SUMMARY

Although correction of path length fluctuations through the complete atmosphere probably cannot be made by measuring backscattered light from a laser beam probe to the accuracy needed for stellar interferometry, it appears that measurements of path lengths can be made over large enough distances to improve such interferometry. The present proposals consider, in particular, corrections over path lengths of 100 m to 1000 m from the ground, where a large fraction of the total path length variations through the atmosphere have been shown to occur at least under some observing conditions. The precision achievable appears adequate to substantially improve interferometry in the mid-IR (10 μm wavelength) region. At optical wavelengths, the precision required is much more demanding, and the distances over which good corrections could be made can be expected to be at least on order of magnitude less that those for the mid-IR region. Nevertheless, some useful corrections might be achieved for wavelengths as short as visible light.

Further study of the nature of path length variations would be appropriate before systems for their correction are completely designed or planned. This might include better knowledge of the relative magnitude and variations of aerosol to molecular scattering near the ground and the relative importance of water vapor concentration variations compared to atmospheric density fluctuations. And further knowledge of the path length fluctuations within 100–1000 m of the ground compared to those in the higher atmospheres would be important. Although uncertainties remain as to the extent of corrections which can reasonably be made, it does appear practical to make partial corrections that can give significant improvements to the quality of stellar interferometry from ground observatories.

This work has been sponsored by the Army Research Office and by the National Science Foundation. I want to also express my special appreciation to John W. Meriwether of Clemson University and Thomas Duck of the Haystack Observatory, Massachusetts Institute of Technology, whose lidar work on the upper atmosphere suggested to me the application of lidar to interferometry, and who helped me with much background information. I also appreciate helpful comments of Professors Edwin Eloranta of the University of Wisconsin and Raymond Measures of the University of Toronto.

REFERENCES

Ansmann, A., Riebesell, M., & Weitkamp, C. 1990, Opt. Lett., 15, 746
Bester, M., Danchi, W. C., Degiacomi, C. G., Greenhill, L. J., & Townes, C. H. 1992, ApJ, 392, 357
Carswell, A. I., Pal, P. R., Streinbrecht, W., Whiteway, J. A., Ulitsky, V., & Wang, T. Y. 1991, Canadian J. Phys., 69, 1076
D'Altorio, S., Masei, F., Rizi, V., Visconti, G., & Verdecchia, M. 1993, Geophys. Res. Lett., 20, 2869
Duck, T. J., Whiteway, J. A., & Carswell, A. J. 1998, Geophys. Res. Lett., 25, 2813
Duck, T. J. 1999, Ph.D. thesis, York Univ., Canada
Gal-Chen, T. M., Xu, M., & Eberhard, W. L. 1992, J. Geophys. Res., 97, 18409
Hale, D. D. S., et al. 2000, ApJ, 537, 998
Measures, R. M. 1984, Laser Remote Sensing—Fundamentals and Applications (New York: Wiley)
Meriwether, J. W., Dao, P. D., McNutt, R. J., Klementi, W., Moskowitz, W., & Davidson, W. 1994, J. Geophys. Res., 99, 16973
Müller, D., Wandinger, U., Althausen, D., Mattis, I., & Ansmann, A. 1998, Appl. Opt., 37, 2260
Pal, S. R., Carswell, A. J., Bird, J., Donavan, D., Duck, T., & Whiteway, J. 1996, Proc. SPIE, 2833, 28
Piironen, P., & Eloranta, E. W. 1994, Opt. Lett., 19, 234
Rothermel, J., Bowdle, D. A., Vaughn, J. M., & Woodfield, A. A. 1991, J. Geophys. Res., 96, 5293
Truehaft, R. N., Lowe, S. T., Bester, M., Danchi, W. C., & Townes, C. H. 1995, ApJ, 453, 522
Whiteman, D. N., Melfi, S. H., & Ferrare, R. A. 1992, Appl. Opt., 31, 3058
Whiteway, J. A., & Carswell, A. J. 1994, J. Atmos. Sci., 51, 3122

Low Altitude Atmospheric Turbulence Characteristics at Mt. Wilson Observatory

Nicholas Short, Walt Fitelson, David Hale, Charles H. Townes

Infrared Spatial Interferometry (ISI) Group
Space Sciences Laboratory
University of California, Berkeley
Berkeley, CA 94704

ABSTRACT

Previous measurements of atmospheric density fluctuations have shown that a substantial fraction of seeing fluctuations occur within 100 feet of the ground,[1] and that the power spectrum of path length fluctuations through the atmosphere has a somewhat smaller slope than that predicted by the Kolmogorov-Taylor approximation.[2] To provide some possibility of appreciable path-length corrections, the ISI has assembled a system capable of measuring temperature changes at fifteen foot intervals of heights up to 70 feet from the ground. Analysis of temperature measurements made under a variety of conditions confirms previous results concerning the decrease in the magnitude of the fluctuations with altitude near the ground: the rms magnitude of the temperature fluctuations at an elevation of 70 feet is, on average, 52% of the mean rms value at 9 feet. However, these new measurements made at point locations show a power spectrum close to the Kolmogorov-Taylor prediction at frequencies up to 1.0 Hz, for average wind speeds above 2 m/s. In addition, correlation analysis between sensors located at the same elevation but separated by a given distance shows up to 50% correlation out to separations as large as 24 meters with wind speeds of a few meters per second, and indicate that Taylor's approximation applies over spatial distances in the range of 24-85 meters, or on timescales as large as ten seconds, and perhaps as large as 14 or 15 seconds. This makes path length corrections possible by temperature measurements at nearby locations.

Keywords: Atmospheric Turbulence, Kolmogorov, Temperature Fluctuations

1. INTRODUCTION

In order to correct for the effects of atmospheric turbulence, it is useful to know the nature of fluctuations in parameters such as temperature or index of refraction, and how well these fluctuations may be determined or correlated. In understanding such atmospheric fluctuations, astronomers typically use Kolmogorov theory to describe the spatial structure of turbulence, in conjunction with the Taylor approximation. Studies conducted by various groups at many different sites have produced results which show both good agreement with[3–5] and significant deviation[2,6,7] from the Kolmogorov-Taylor (KT) theoretical description of the atmosphere. This study presents the results of analyzing temperature fluctuations made on several nights between March of 2001 and January of 2002, at various heights above the ground, at the Infrared Spatial Interferometer (ISI) site at Mt. Wilson Observatory.

This paper is organized as follows. Section 2 briefly describes the system used to measure temperature fluctuations for this study. Section 3 then reviews the KT theoretical description of the atmosphere, and presents some of the analytical methods useful for investigating the nature of atmospheric parameters, including the structure function and the related power spectrum. The remaining sections, 4 through 6, present the results of various types of analysis performed on the data gathered with this system. Section 4 presents the results of analyzing the power spectra of the temperature measurements. Specifically, values of the slope are determined

Further author information:
Nicholas Short: E-mail: nick@ssl.berkeley.edu, Telephone: 1-510-642-9500
Charles H. Townes: E-mail: cht@ssl.berkeley.edu, Telephone: 1-510-642-7686

Interferometry for Optical Astronomy II, Wesley A. Traub, Editor,
Proceedings of SPIE Vol. 4838 (2003) © 2003 SPIE · 0277-786X/03/$15.00

over various frequency ranges and the results are compared to the values predicted by Kolmogorov-Taylor theory. Section 5 examines changes in the rms value of the temperature fluctuations, and presents any observed dependence of the rms value on wind speed, time of night, and altitude. Finally, section 6 looks at the peak values and time delays of the cross correlation between sensors separated horizontally.

2. INSTRUMENTATION

In order to measure the temperature precisely at different elevations, five Type E chrome-constantan thermocouples were mounted at different elevations on a telescoping mast. The mast sections were elevated to approximately 9, 24, 39, 54, and 70 feet, giving temperature readings every 15 ft within the first 70 feet of the atmosphere. For the rest of this paper, sensor 1 will refer to the lowest thermocouple located at 9 feet, and sensor 5 will refer to the uppermost thermocouple located at 70 feet. A Campbell CR10X data logger measured the differential voltage of each thermocouple, the wind speed and direction of a wind anemometer located on top of the mast, and the temperature of a reference thermistor located in the data logger. The wind speed was read only once a second, while the other values were all sampled at a frequency of 22 Hz.* In order to calculate the correlation between sensors at various spatial separation, two telescoping masts containing identical systems were used to monitor how the temperature behaves at various locations of the Infrared Spatial Interferometer (ISI) site at Mt. Wilson Observatory. The raw data for analysis contained five temperature readings in degrees Celsius at the abovementioned elevations, as well as wind speed in meters per second and wind direction in degrees, sampled continuously in time. A typical data set contains approximately 45 minutes of data.

3. THEORETICAL CONSIDERATIONS

Atmospheric turbulence has been generally described as having a Kolmogorov spatial structure. In this theory, it is assumed that large scale spatial motions are subsequently transferred to small scale motions, and that these processes occur in a random fashion. The resulting spatial distribution of various atmospheric parameters such as temperature, index of refraction, or wind speed is consequently assumed to be both homogeneous and isotropic. Using these assumptions, Kolmogorov and others produced a mathematical description of the variation in such parameters as a function of spatial separation. Variations as a function of time for a fixed point in space use the Kolmogorov-Taylor approximation, which assumes that atmospheric density fluctuations all move simultaneously with the wind. By comparing predictions of this model with the results of measurements of real temperature fluctuations, one can determine the extent to which the atmosphere above Mt. Wilson Observatory behaves like the ideal KT model.

There are several ways of analyzing variations in temperature or the index of refraction, of which the structure function, both spatial and temporal, and the power spectrum are perhaps the most useful. Present experiments measure small and rapid changes in temperature, and the fractional change is assumed to be the same as that for denisty or index of refraction. This assumption is safe under conditions where the pressure remains relatively constant, since $n = C\frac{P}{T}$, and subsequently:

$$\frac{dn}{dt} = C\frac{1}{T}\frac{dP}{dt} - C\frac{P}{T^2}\frac{dT}{dt}. \tag{1}$$

where C is some constant of proportionality.

The spatial structure function of a variable such as the index of refraction, n, is defined as

$$D_n(r) = < [n(r_2) - n(r_1)]^2 > \tag{2}$$

where r_i represents a position vector and $D_n(r)$ represents an ensemble average for all points separated by a distance $r = |r_2 - r_1|$. Typically, spatial structure functions for atmospheric fluctuations are assumed to have a form

$$D_n(r) = C_n^2 r^\alpha \tag{3}$$

*For optical wavelengths, atmospheric fluctuations of importance can be faster than 22 Hz, but for wavelengths in the 10 micron region where the ISI is used, fluctuations faster than 22 Hz are small enough to generally be insignificant.

over certain limited distance ranges, where C_n and α represent the coefficients to be determined.

In order to convert this spatial structure function to a temporal structure function, we have to make some sort of assumption about the temporal behavior of the atmosphere. The most commonly used approximation for this purpose is the Taylor approximation, which assumes that the Kolmogorov spatial variations are "blown" from one point in space to another by wind at a constant velocity V. Using this approximation, the spatial structure function (Equation 3) can be converted to a temporal structure function by noting that $t = r/V$.

$$D_n(r) = C_n^2 V^\alpha t^\alpha \tag{4}$$

Kolmogorov-Taylor theory predicts $\alpha = 2/3$ at relatively short times (thousandths to tenths of a second) for a temporal structure function of temperature fluctuations, leveling off to $\alpha = 0$ at longer times (hundreds to thousands of seconds). The turning point, where the structure function changes from obeying one power law to another, occurs at time $t = L_k/V$, where L_k represents the outer scale of turbulence, or the spatial limit to which Kolmogorov's assumptions apply.

Much like the temporal structure function, the power spectrum of the density fluctuations also behaves according to theoretically determined power laws, exhibiting a temporal frequency dependence of ν^β. According to KT theory, for measurements taken at a point source, $\beta = -5/3$ in high frequency ranges, while in low frequency ranges $\beta = 0$. The turning point, in this case, occurs at a temporal frequency of $\nu = V/L_k$. For measurements made over a path in the atmosphere, $\beta = -8/3$ in high frequency ranges, while in low frequency ranges $\beta = 0$. In a sense, both the temporal structure function and the power spectrum contain the same information. In this paper we focus on analyzing the power spectrum of measured temperature fluctuations.

4. POWER SPECTRUM ANALYSIS

For each 25 minute segment of data, the power spectral density was computed in the usual fashion. Before calculating the slope of the individual spectra by doing a least squares fit over certain designated frequency ranges, the mean value of the noise floor was subtracted from each spectrum and the result was multiplied by a frequency dependent correction factor of

$$1 + (\omega\tau)^2 \tag{5}$$

to correct for the observed time constant response of the thermocouples. In the above equation, $\omega = 2\pi\nu$ where ν is the temporal frequency, and τ is the time constant in seconds, which was measured to be roughly 35 milliseconds. A typical power spectrum, before and after noise floor subtraction and time constant correction is shown in Figure 1. The average wind speed during this particular data set was 3.90 m/s.

In order to get a statistical sense of how these spectral slopes vary with altitude and wind speed, the average values of the slopes were tabulated for each sensor, in each frequency range, with various average wind speeds over the course of the data sets. Tables 1 through 3 in Appendix A of this paper show the results of this tabulation for each of three frequency ranges: 0.001 to 0.01 Hz, 0.01 to 0.1 Hz, and 0.1 to 1.0 Hz. Shown with the average slope is the standard deviation from the average value, as well as the number of data sets averaged, shown in parentheses. Several trends are apparent in these tables.

First, the slopes for the lowest frequency ranges, 0.001 to 0.01 Hz (Table 1), show an average standard deviation on the order of, and sometimes greater than, the mean value of the slope itself. This statistically confirms what is visually evident in Figure 1: at the lower frequency ranges, the power spectra rarely behave as simply as Kolmogorov-Taylor theory predicts. However, despite the large variation in slope values, at each given altitude the average slopes do increase, or become less negative, with increasing wind speed. For example, the average spectral slope for sensor 3 increases from -1.72 to -0.62 as the wind increases from 0.5 to 6.5 m/s, though the standard deviation is consistently about +/- 0.60. Interestingly, this trend also occurs for spectral slopes in higher frequency ranges (discussed below).

As mentioned in Section 3, the turning point or breakpoint between theoretical spectral power laws is dependent upon wind speed, being equal to V/L_k . If the outer scale L_k remains constant, then an increase in wind speed has the general effect of moving the breakpoint to higher frequency values. This may partially explain the increase in spectral slope value at higher wind speeds between 0.001 and 0.01 Hz, since at very low

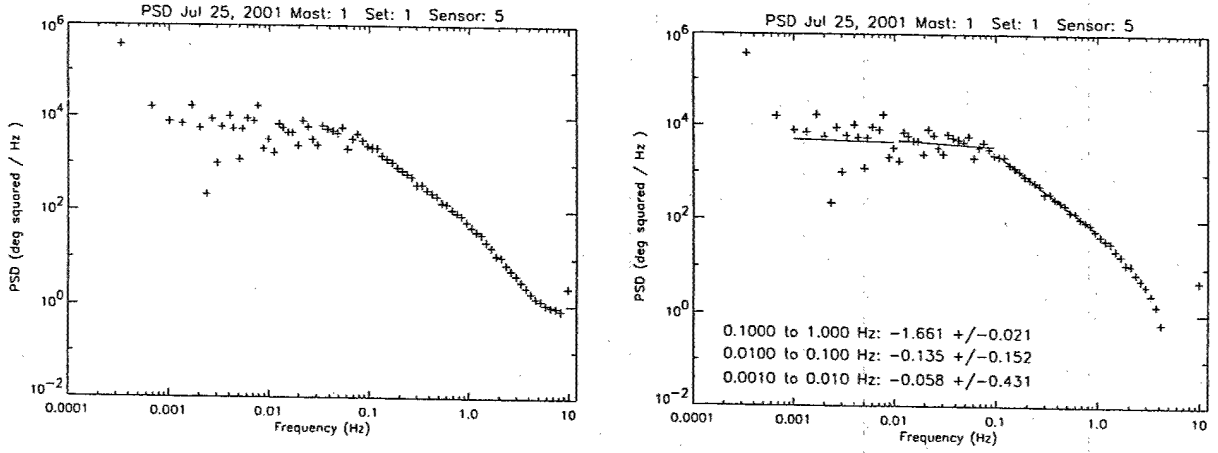

Figure 1. A Typical Logarithmic Power Spectrum. In both figures, the spectra are averaged so the points appear equally spaced when plotted logarithmically. The figure on the left shows the spectrum before noise floor subtraction and time constant correction. The figure on the right shows the spectrum after these operations have been performed. In addition, in the figure on the right, lines obtained by least squares fitting the data over designated frequency ranges are plotted, and the slope of each line is printed in the lower left-hand corner along with the standard deviation of the points from each fit.

wind speeds the power spectra may still follow the -5/3 theoretical approximation down to frequencies as low as a thousandth of a Hz. Another possibility is that the spectra, after flattening out, begin to rise again, a phenomenon which has been observed in some spectra.

In the next frequency interval (shown in Table 2), from 0.01 to 0.1 Hz, the average slopes still have substantial standard deviations though they are smaller than those observed in the lowest frequency range implying that while there is still substantial variations in the fit, the spectral slope values are not as random as those shown in Table 1. In addition, the slopes in a given range of wind speeds do not appear to have any dependency on altitude. However, at a fixed altitude the slopes do seem to increase or become less negative, on average, with increasing wind speed up to speeds of 6 m/s, with the exception of sensor 1. Sensor 1, because it is located only 9 feet above the ground, is believed to behave the least like the KT theoretical prediction, which assumes no boundary conditions, and so its exceptionality in this cause is not too surprising.

At the highest range of frequencies, from 0.1 to 1.0 Hz (Table 3), the power spectral slopes at a given altitude also seem to increase or become less negative with increasing wind speed. This is evident in sensor 1, where the average slope decreases from -1.70 to -1.44 as the wind speed increases from 2.5 to 6.5 m/s, as well as sensor 5 where the slope decreases from -1.60 to -1.46 over the same range of wind speeds.[†]. In addition, at the highest range of frequencies, the spectral slopes in a given wind speed range seem generally to increase, or become less negative, as the height increases, at least for wind speed ranges above 2 m/s and below 5 m/s. For example, in the wind speed range of 3.0 to 4.0 m/s, the slope increases from -1.74 at sensor 1 to -1.58 at sensor 5. This general trend toward smaller slopes at larger elevations may be due to gradients in wind speed within the low-level atmosphere. Above 5 m/s in wind speed, this general trend is not so apparent, and the slopes tend to show constant values, in a given range of wind speeds, at all five elevations. This suggests that gradients in wind speed at these elevations are reduced at higher average speeds.

At wind speeds below 2 m/s, the trends mentioned above are not so apparent, and generally speaking, the spectral slopes between 0.1 and 1.0 Hz behave least like the KT prediction at low altitudes and at low wind speeds. Visual inspection of the spectra shows that at slow wind speeds, the noise floor begins closer to 1 Hz than 7 or 8 Hz, which is typical of higher wind speeds (see Figure 1). Since the range of frequencies fitted, in this case, comes so close to the beginning of the noise floor, the derived slopes may be unduly steepended by

[†]The last wind speed range, 7 to 8 m/s, is ignored here since it contains only one point and does not represent a suitable average

the noise floor subtraction. Deviations from theoretical prediction of -1.66 at higher elevations and larger wind speeds may reflect the dependency of the spectral turning point on average wind speed when the outer scale is assumed to be constant. Though this type of analysis does not provide for a precise determination of the value of the outer scale, it can be roughly estimated from visual inspection of spectra like the one shown in Figure 1. The turning point in this spectra appears to lie around 0.77 Hz, which for a wind speed of 3.90 m/s suggests and outer scale of approximately 50 meters. However, the wind speeds considered in this data only vary from 0.5 to 8.5 m/s, roughly a factor of ten, and so cannot entirely explain a variation in the frequency value of the spectral turning point of at least a factor of one hundred (recall that slopes of -5/3, albeit with large standrad deviations, are observed at frequencies as low as 0.001 Hz for low wind speeds). Thus, the value of the outer scale may also vary with conditions, something we intend to investigate further in the future.

5. RMS VALUES OF THE TEMPERATURE FLUCTUATIONS

While a discussion of power spectral slopes for temperature readings allows a comparison with KT theory, it is also useful to know how the magnitude of variations in temperature, and hence variations in index of refraction and phase, change with altitude. Analysis of the root mean square (rms) value of the temperature fluctuations is useful in this respect, and was performed as follows.

For each set of temperature readings, a running mean (or boxcar average) of 60 second width was subtracted to remove the long timescale, low frequency variations since fluctuations on these timescales do not substantially contribute to distortions in phase or path length in interferometric observation of starlight in the infrared. The data set was then broken into smaller five minute segments, and for each five minute segment the rms value of the temperature fluctuations in degrees Celsius was calculated, in addition to the average wind speed and the relative time of night[‡]. The rms values of the temperature fluctuations were then plotted, for each sensor, as a function of these two variables. Figure 2 shows these plots for sensors 1, 3, and 5. In addition, tables 4 and 5 show the mean rms value of the temperature fluctuations for each sensor tabulated as a function of average wind speed and relative time of night. The numbers in parantheses in these tables indicate the number of points averaged.

Though the rms values are fairly scattered in the plot on the left in Figure 2, at the higher elevations and at the lower speeds one can see that the rms values do increase with wind speed. This is also evident in the tabulation of these values. For example, as shown in Table 4, the average rms values for sensor 4 increase from 0.08 to 0.19 degrees C as the average wind speed increases from 0.5 to 2.5 m/s. The rms values then remain relatively constant at this altitude with increasing wind speed, with the exception of the highest wind speed range (7.0 to 8.0 m/s), which may not represent as complete of an average since only 22 data sets have average speeds within this range. The trend is not so noticeable towards the bottom of the mast, where ground effects generally cause the wind to blow slower than at the top of the mast where the wind speed is measured.

The rms values also seem to decrease with increasing altitude, except at the highest wind speeds. For example, as shown in Fig 4, the average rms value for data sets with wind speeds between 1 and 2 m/s decreases from 0.25 degrees C at sensor 1 to 0.10 degrees C at sensor 5. Similar trends can be seen at different wind speed bins, with the exception of the highest (7.0 to 8.0 m/s). Averaging over all values of wind speed, the mean rms value for the temperature fluctuations of sensor 1 is 0.25 degrees C, while for sensor 3 it is 0.19 degrees C, and for sensor 5 it is only 0.13 degrees C. Thus, averaging over a wide variety of atmospheric conditions, the mean rms magnitude of the temperature fluctuations at an altitude of 70 feet is 52% of the mean rms value at an altitude of only 9 feet.

The plot on the right in Figure 2, and the values presented in Table 5, show changes in the rms values with respect to relative time of night. It has often been hypothesized that sunrise and sunset (0 and 1 on the relative time scale) offer the best possible seeing conditions since the atmosphere is the most stable, or the least turbulent, at these times. This phenomenon should be reflected in smaller average rms values at these times. The figure seems to show a series of rises and falls, though this may simply be the result of having more data in certain ranges of relative time. In addition, the averaged values presented in Table 5 do not show any drastic

[‡]Relative time of night refers to a fractional time scale from sunset (value of 0) to sunrise (value of 1).

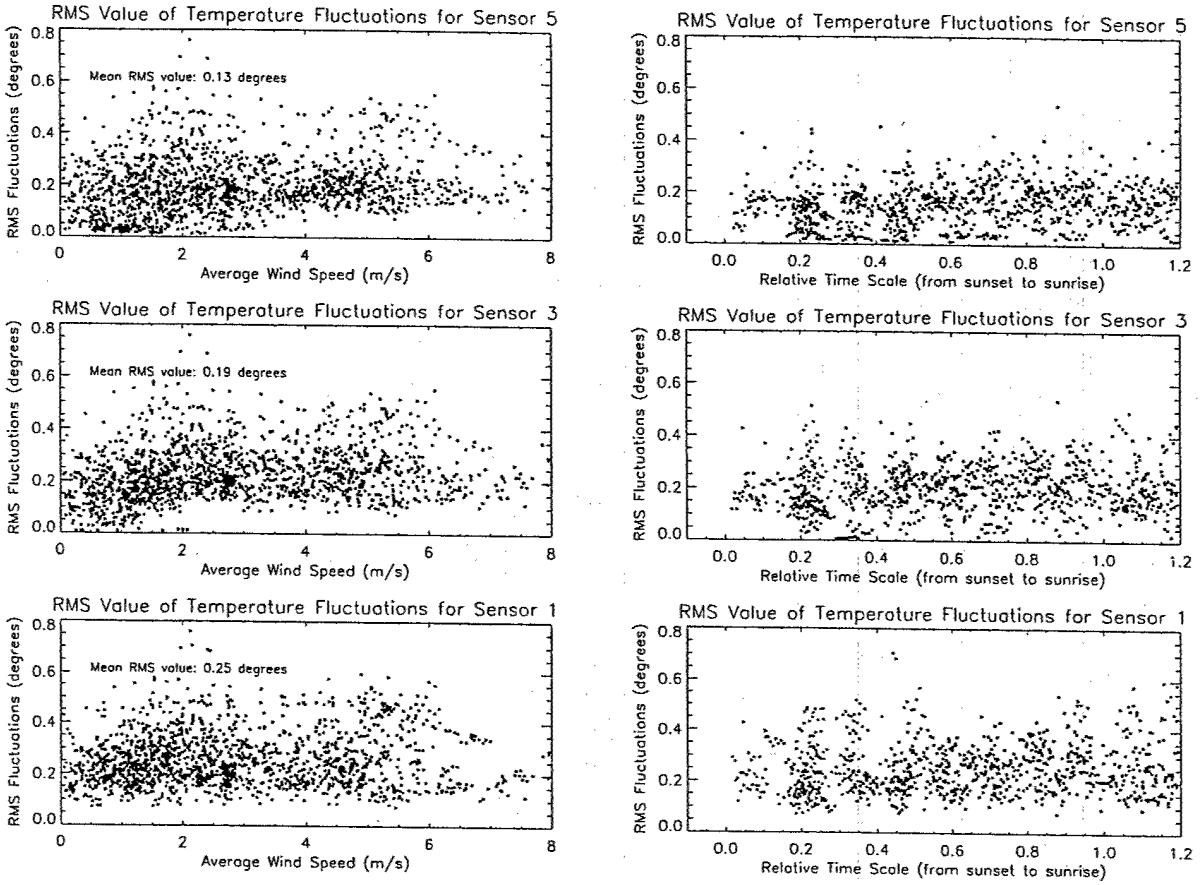

Figure 2. RMS value of the temperature fluctuations from 15 different nights of data, plotted as a function of average wind speed (left) and relative time of night (right) for sensors 5, 3, and 1 (at altitudes of 70, 39, and 9 feet respectively). The mean rms value, averaged over all conditions for a given sensor, is printed in the plot on the left showing that the average rms value drops by roughly a factor of two from 9 feet (sensor 1) to 70 feet (sensor 5). The plot on the right shows that same data as that on the left, but plotted as a function of relative time, a fractional time scale from sunset (which corresponds to 0) and sunrise (which corresponds to 1).

changes close to sunrise and sunset. This suggests that, while such a relationship may exist, the rms value of the temperature fluctuations is more dependent on overall wind speed than on time of night.

6. CORRELATION ANALYSIS

To test the Taylor hypothesis and to determine the distance scales on which Taylor's approximation remains accurate, it is useful to examine the cross correlation of sensors separated horizontally, or sensors at the same elevation but on different masts. Recall that the Taylor approximation assumes temperature fluctuations are "frozen" in the atmosphere and are blown from one point to another by a wind of constant velocity, V (see Section 3).

The general method used in computing the correlations is as follows. Before calculating the cross correlation, a running mean (or boxcar average) of 30 second width was subtracted from the temperature readings of each data set in order to remove the contribution of long timescale fluctutations which are not so relevant to our inquiry. Each data set was then shortened to segments of 10 minute length, and the correlation coefficient between two different sensors was computed out to +/- 100 seconds on a delayed time axis.

For each correlation curve, the following was recorded: the average wind speed and direction for the data set concerned, the peak value of the correlation coefficient, the lag or delayed time value at which the correlation

curve peaks, and the kurtosis of the curve. The kurtosis of each correlation curve was recorded as a numerical way of gauging the "peakedness" of a given curve relative to a normal distribution. As the fourth statistical moment, the kurtosis is defined as:

$$Kurt(x_1 \ldots x_n) = \{\frac{1}{N}\sum_{j=1}^{N}[\frac{x_j - \overline{x}}{\sigma}]\} - 3 \tag{6}$$

where the -3 makes the value zero for a normal distribution.[8] A negative value for the kurtosis indicates relative "flatness", while a positive value indicates strong "peakedness". Imposing a minimum kurtosis value of 1.0 on the data generally eliminates curves with peak values in the range of 0.2 which, in the analysis that follows, should be considered a poor correlation. In the data presented here, a minimum kurtosis value of 0.01 was imposed, essentially eliminating those sets that had a negative kurtosis.

In the fifteen nights of data analyzed in this section, the masts were separated by distances ranging from a couple of feet to approximately 24.3 meters. To account for the wide variety of separations and wind conditions, the correlation peak values and time delays are all plotted as a function of the estimated time delay. The estimated time delay is calculated from the wind measurement, and is defined as the horizontal separation (in meters) divided by the component of the wind speed in the direction of the separation (in meters per second).

Figure 3 shows the value of the horizontal correlation peaks as a function of estimated time delay for sensors 5 and 2. Both plots only show data in which the wind was blowing at least 80% in the direction of separation (or, in terms of degrees, within 36.7 degrees of the direction of separation on average). The x axis is plotted logarithmically, and so the roughly linear relationship in the plot suggests an approximately exponential decrease in correlation coefficient as a function of time delay. If we assume 0.5 or 50% correlation represents a significant correlation, then as the plot for sensor 5 (left) shows, significant correlation exists out to time delays of approximately 9-10 seconds. The plot for sensor 2 shows similar results, though the magnitude of the correlations are generally smaller, and 50% correlation can be seen out to times only as large as 5 seconds. The data for sensor 1, though not plotted here, show little correlation on timescales larger than 2 seconds.

This data can provide a rough estimate of the range of spatial distances for which Taylor's approximation is accurate. Since 50% correlation is observed out to delayed times of approximately 10 seconds for sensor 5 (where the wind speed and direction is measured), then given the range of wind speeds we have considered, 0 to 8.5 m/s, we know that Taylor's approximation could be accurate out to separations as large as 85 meters. Correlation coefficient values of 0.5 have been observed at separations as large as 24 meters, with the wind

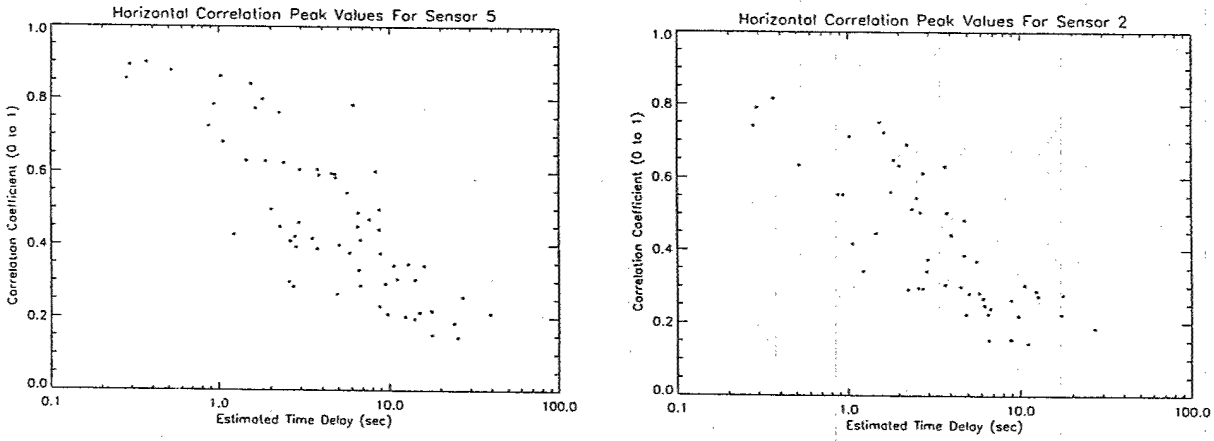

Figure 3. Peak values for horizontal correlations between two sensors at the same elevation, but on different masts separated by distances between 1 and 24 meters. The data presented here shows the results for sensor 5 (left) and sensor 2 (right), and shows only those data sets when the wind was blowing at least 80% in the direction of separation of the sensors.

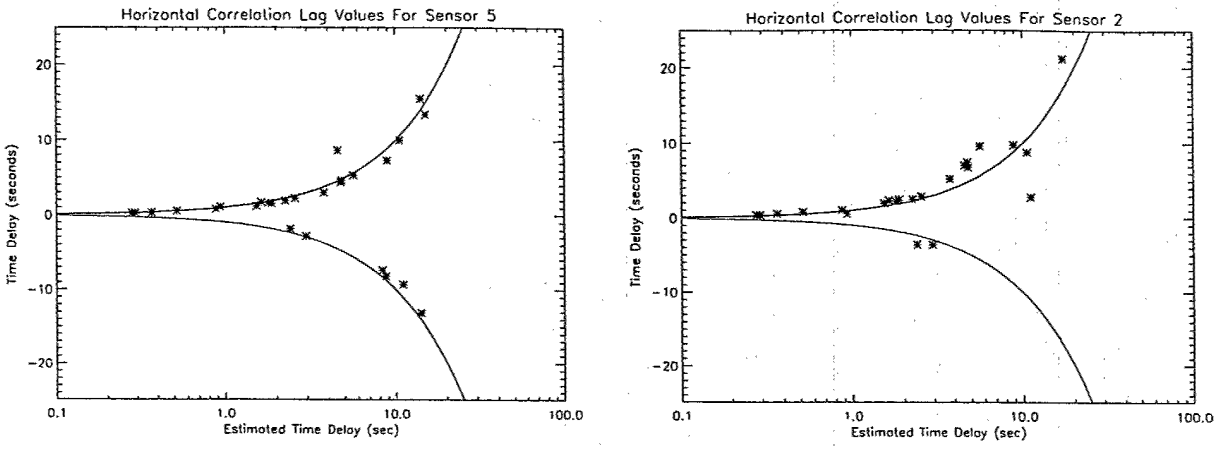

Figure 4. The observed time delay between sensor 5 on both masts (left) and sensor 2 on both masts (right), when the masts are separated by various distances. The wind was blowing at least 93% in the direction of separation of the sensors in the data presented here. The solid line indicates the expected value of the time delay derived from measurements of the wind speed and direction.

blowing approximately 80% in the direction of separation. Thus, we know the approximation remains accurate out to distances of 20 meters, and it is possible that it could remain accurate out to distances of roughly four times that value, depending on the conditions. Another way of looking at it is that for elevations of 24 feet and above, Taylor's approximation remains accurate on a characteristic timescale of zero to five or ten seconds, after which any instantaneous temperature fluctuation is not accurately predicted by the Taylor "frozen-atmosphere" model.

A comparison of the observed time delay, the time delay value at which the correlation curve reaches its maximum value, with respect to the time delay estimated from the wind measurement provides another way of testing Taylor's hypothesis. If Taylor's atmospheric model is accurate, then the observed delay time should be close to the values estimated from distance and wind speed.

Figure 4 shows the observed time delay between two sensors at the same elevation, plotted as a function of the estimated time delay. The wind was blowing at least 93% in the direction of separation of the masts in the data presented here, and results are shown for two different elevations, that of sensor 5 (left) and sensor 2 (right). The solid lines in both figures show the estimated value of the time delay, derived from measurements of the wind speed, direction, and distance of separation. As shown, the observed time delay agrees fairly well with the estimated values. Though error bars were left off of the plot, all of the observed values shown in Figure 4 do fall within one standard deviation of the estimated value[§]. In addition, several data sets show good correlation out to time delays of 14-15 seconds, suggesting that for sensor 5, Taylor's approximation may remain valid on timescales slightly larger than indicated from the analysis of correlation peak values above. The time delay values observed for sensor 2 are generally larger in magnitude than those of sensor 5 and than those calculated from wind speed, perhaps because of slower wind speeds closer to the ground.

7. CONCLUSION

Analysis of the power spectral slopes of temperature fluctuations within 70 feet of the ground show good agreement with the Kolmogorov-Taylor theoretical predictions for frequencies between 0.1 and 1.0 Hz, when averaged over a variety of conditions. For example, averaging over all wind speeds for each sensor in Table 3 produces mean slopes of -1.64, -1.62, -1.60, -1.56, and -1.58 for sensor 1 through 5, respectively. Averaging only over wind speeds between 0 and 4 m/s produces mean slopes of -1.75, -1.71, -1.67, -1.59, and -1.66. Thus, the

[§]The standard deviation, in this case, was determined by multiplying the horizonal separation by the standard deviation of the inverse of the component of the wind speed in the direction of separation

slopes agree well with the KT predictions at altitudes of 39 feet (sensor 3) and above at conditions of low wind speeds (below 4 m/s). Averaging over all conditions, the spectral slopes at all elevations below 70 feet tend to be slightly smaller (or less negative) than the theoretical value of -5/3, perhaps because of the relationship between wind speed and the "turning point" between logarithmic power laws when the outer scale is held constant.

Analysis of the rms value of the temperature fluctuations on short timescales (less than 60 seconds) shows that the magnitude of the rms fluctuations decreases by 52% between elevations of 9 and 70 feet when averaged over a variety of conditions. Furthermore, correlation analysis of sensors located at the same elevation but separated by various fixed horizontal distances shows that the Taylor approximation remains valid on timescales of at least ten, and perhaps fifteen, seconds. Since Taylor's hypothesis remains accurate on these timescales, and since a substantial fraction of temperature, and hence index of refraction, variations occur within the first seventy feet of the atmosphere, significant path length correction is possible by making high speed temperature measurements at locations close to individual telescopes.

APPENDIX A. TABULATION OF POWER SPECTRA SLOPES

Table 1. Power spectrum slopes obtained from least squares fitting individual spectra in the range of frequencies from 0.001 to 0.01 Hz, tabulated as a function of average wind speed. The average standard deviation of the points from each fit follows the mean value of the slope for all data sets in the given range of wind speeds, as well as the number of data sets averaged in parantheses. Sensors 1 through 5 are at elevations of 9, 24, 39, 54, and 70 feet respectively.

Wind Speed	sensor: 1	2	3
0.0 to 1.0	-1.66 +/- 0.61 (18)	-1.57 +/- 0.58 (18)	-1.72 +/- 0.61 (18)
1.0 to 2.0	-1.20 +/- 0.75 (33)	-1.28 +/- 0.76 (33)	-1.39 +/- 0.83 (33)
2.0 to 3.0	-1.13 +/- 0.59 (22)	-1.29 +/- 0.57 (22)	-1.34 +/- 0.56 (22)
3.0 to 4.0	-0.73 +/- 0.57 (11)	-0.76 +/- 0.46 (11)	-0.77 +/- 0.46 (11)
4.0 to 5.0	-0.96 +/- 0.68 (17)	-1.10 +/- 0.74 (17)	-0.86 +/- 0.68 (17)
5.0 to 6.0	-0.59 +/- 0.84 (10)	-0.83 +/- 0.43 (10)	-0.85 +/- 0.56 (10)
6.0 to 7.0	-0.52 +/- 0.88 (5)	-0.74 +/- 0.51 (5)	-0.62 +/- 0.63 (5)
7.0 to 8.0	-0.45 +/- NaN (1)	-0.46 +/- NaN (1)	-0.40 +/- NaN (1)

Wind Speed	sensor: 4	5	
0.0 to 1.0	-1.98 +/- 0.80 (18)	-2.01 +/- 0.58 (18)	
1.0 to 2.0	-1.48 +/- 0.76 (33)	-1.50 +/- 0.77 (33)	
2.0 to 3.0	-1.33 +/- 0.67 (22)	-1.54 +/- 0.88 (22)	
3.0 to 4.0	-0.77 +/- 0.39 (11)	-0.80 +/- 0.77 (11)	
4.0 to 5.0	-0.76 +/- 0.75 (17)	-0.78 +/- 0.91 (17)	
5.0 to 6.0	-0.88 +/- 0.62 (10)	-0.78 +/- 0.55 (10)	
6.0 to 7.0	-0.18 +/- 1.27 (5)	-0.27 +/- 0.78 (5)	
7.0 to 8.0	-0.15 +/- NaN (1)	-0.19 +/- NaN (1)	

Table 2. Power spectrum slopes obtained from least squares fitting individual spectra in the range of frequencies from 0.01 to 0.1 Hz, tabulated as a function of average wind speed.

Wind Speed	sensor: 1	2	3
0.0 to 1.0	-0.81 +/- 0.43 (18)	-0.96 +/- 0.29 (18)	-0.96 +/- 0.40 (18)
1.0 to 2.0	-1.04 +/- 0.28 (33)	-0.99 +/- 0.33 (33)	-0.97 +/- 0.21 (33)
2.0 to 3.0	-0.79 +/- 0.27 (22)	-0.70 +/- 0.30 (22)	-0.53 +/- 0.37 (22)
3.0 to 4.0	-0.77 +/- 0.31 (11)	-0.65 +/- 0.30 (11)	-0.71 +/- 0.26 (11)
4.0 to 5.0	-0.82 +/- 0.29 (17)	-0.73 +/- 0.28 (17)	-0.59 +/- 0.40 (17)
5.0 to 6.0	-0.79 +/- 0.49 (10)	-0.64 +/- 0.37 (10)	-0.64 +/- 0.36 (10)
6.0 to 7.0	-0.86 +/- 0.36 (5)	-0.70 +/- 0.60 (5)	-0.81 +/- 0.39 (5)
7.0 to 8.0	-1.03 +/- NaN (1)	-0.98 +/- NaN (1)	-1.01 +/- NaN (1)
Wind Speed	sensor: 4	5	
0.0 to 1.0	-1.12 +/- 0.19 (18)	-1.21 +/- 0.22 (18)	
1.0 to 2.0	-1.03 +/- 0.19 (33)	-1.00 +/- 0.27 (33)	
2.0 to 3.0	-0.66 +/- 0.36 (22)	-0.88 +/- 0.39 (22)	
3.0 to 4.0	-0.66 +/- 0.19 (11)	-0.64 +/- 0.21 (11)	
4.0 to 5.0	-0.61 +/- 0.39 (17)	-0.65 +/- 0.43 (17)	
5.0 to 6.0	-0.57 +/- 0.36 (10)	-0.76 +/- 0.39 (10)	
6.0 to 7.0	-0.96 +/- 0.29 (5)	-1.12 +/- 0.16 (5)	
7.0 to 8.0	-1.01 +/- NaN (1)	-1.14 +/- NaN (1)	

Table 3. Power spectrum slopes obtained from least squares fitting individual spectra in the range of frequencies from 0.1 to 1.0 Hz, tabulated as a function of average wind speed.

Wind Speed	sensor: 1	2	3
0.0 to 1.0	-1.81 +/- 0.14 (18)	-1.74 +/- 0.15 (18)	-1.63 +/- 0.25 (18)
1.0 to 2.0	-1.76 +/- 0.17 (33)	-1.68 +/- 0.15 (33)	-1.70 +/- 0.14 (33)
2.0 to 3.0	-1.70 +/- 0.11 (22)	-1.66 +/- 0.10 (22)	-1.67 +/- 0.09 (22)
3.0 to 4.0	-1.74 +/- 0.21 (11)	-1.75 +/- 0.15 (11)	-1.68 +/- 0.08 (11)
4.0 to 5.0	-1.64 +/- 0.15 (17)	-1.65 +/- 0.15 (17)	-1.62 +/- 0.12 (17)
5.0 to 6.0	-1.54 +/- 0.15 (10)	-1.53 +/- 0.07 (10)	-1.55 +/- 0.09 (10)
6.0 to 7.0	-1.44 +/- 0.06 (5)	-1.44 +/- 0.06 (5)	-1.47 +/- 0.09 (5)
7.0 to 8.0	-1.49 +/- NaN (1)	-1.52 +/- NaN (1)	-1.45 +/- NaN (1)
Wind Speed	sensor: 4	5	
0.0 to 1.0	-1.48 +/- 0.32 (18)	-1.71 +/- 0.30 (18)	
1.0 to 2.0	-1.65 +/- 0.14 (33)	-1.75 +/- 0.23 (33)	
2.0 to 3.0	-1.59 +/- 0.08 (22)	-1.60 +/- 0.10 (22)	
3.0 to 4.0	-1.65 +/- 0.14 (11)	-1.58 +/- 0.07 (11)	
4.0 to 5.0	-1.58 +/- 0.11 (17)	-1.55 +/- 0.09 (17)	
5.0 to 6.0	-1.53 +/- 0.08 (10)	-1.55 +/- 0.11 (10)	
6.0 to 7.0	-1.48 +/- 0.11 (5)	-1.46 +/- 0.13 (5)	
7.0 to 8.0	-1.54 +/- NaN (1)	-1.42 +/- NaN (1)	

APPENDIX B. TABULATION OF RMS VALUES

Table 4. Tabulation of RMS temperature values according to average wind speed. The data presented here was taken from 15 different nights. The rms values are obtained from five minute segments of data after subtraction of a running mean, and the the numbers in parentheses show the total number of sets averaged. Sensors 1 through 5 are at elevations of 9, 24, 39, 54, and 70 feet respectively.

Wind Speed	sensor: 1	2	3	4	5
0.0 to 1.0	0.21 (230)	0.16 (230)	0.10 (230)	0.08 (230)	0.08 (230)
1.0 to 2.0	0.25 (390)	0.20 (390)	0.16 (390)	0.13 (390)	0.10 (390)
2.0 to 3.0	0.26 (306)	0.23 (306)	0.23 (306)	0.19 (306)	0.13 (306)
3.0 to 4.0	0.24 (184)	0.23 (184)	0.22 (184)	0.18 (184)	0.15 (184)
4.0 to 5.0	0.25 (226)	0.25 (226)	0.24 (226)	0.21 (226)	0.18 (226)
5.0 to 6.0	0.30 (152)	0.26 (152)	0.23 (152)	0.20 (152)	0.18 (152)
6.0 to 7.0	0.25 (56)	0.21 (56)	0.19 (56)	0.19 (56)	0.18 (56)
7.0 to 8.0	0.18 (22)	0.20 (22)	0.21 (22)	0.24 (22)	0.25 (22)

Table 5. Tabulation of RMS temperature values according to relative time of night. Relative time is a fractional timescale where a value of 0 corresponds to sunset, and a value of 1 to sunrise.

Relative Time	sensor: 1	2	3	4	5
0.0 to 0.1	0.20 (56)	0.18 (56)	0.16 (56)	0.17 (56)	0.13 (56)
0.1 to 0.2	0.22 (86)	0.20 (86)	0.17 (86)	0.15 (86)	0.13 (86)
0.2 to 0.3	0.23 (222)	0.19 (222)	0.17 (222)	0.14 (222)	0.11 (222)
0.3 to 0.4	0.25 (158)	0.19 (158)	0.18 (158)	0.15 (158)	0.11 (158)
0.4 to 0.5	0.23 (170)	0.22 (170)	0.20 (170)	0.14 (170)	0.12 (170)
0.5 to 0.6	0.26 (152)	0.24 (152)	0.20 (152)	0.17 (152)	0.14 (152)
0.6 to 0.7	0.24 (134)	0.23 (134)	0.20 (134)	0.16 (134)	0.13 (134)
0.7 to 0.8	0.26 (124)	0.22 (124)	0.21 (124)	0.19 (124)	0.15 (124)
0.8 to 0.9	0.27 (130)	0.24 (130)	0.22 (130)	0.18 (130)	0.16 (130)
0.9 to 1.0	0.28 (130)	0.25 (130)	0.22 (130)	0.19 (130)	0.16 (130)
1.0 to 1.1	0.28 (106)	0.23 (106)	0.21 (106)	0.17 (106)	0.14 (106)
1.1 to 1.2	0.27 (96)	0.22 (96)	0.18 (96)	0.15 (96)	0.13 (96)

ACKNOWLEDGMENTS

This work has been supported by the United States Army Research Office.

REFERENCES

1. R. N. Treuhaft and S. T. Lowe, "Vertical scales of turbulence at the Mount Wilson Observatory," *ApJ* **453**, pp. 522–531, 1995.
2. M. Bester, W. Danchi, C. Degiacomi, L. Greenhill, and C. Townes, "Atmospheric fluctuations: Empirical structure functions and projected performance of future instruments," *ApJ* **392**, pp. 357–374, 1992.
3. M. Colavita, M. Shao, and D. H. Staelin, "Atmospheric phase measurements with the Mark III stellar interferometer," *Appl. Opt.* **26**, pp. 4106–4112, 1987.
4. N. Nightingale and D. Buscher, "Inteferometric seeing measurements at the La Palma Observatory," *Mon. Not. R. Astr. Soc.* **251**, pp. 155–166, 1991.
5. D. W. et al., "Characteristics of turbulence measured on a large aperture," *Proc. SPIE* **9226**, pp. 360–366, 1988.
6. D. Acton, R. Sharbaugh, J. Roehrig, and D. Tiszauer, "Wave-front tilt power spectral density from the image motion of solar pores," *Appl. Opt.* **31**, pp. 4280–4284, 1992.
7. R. Linfield, M. Colavita, and B. Lane, "Atmospheric turbulence measurements with the Palomar Testbed Interferometer," *ApJ* **554**, pp. 505–513, 2001.
8. W. H. Press, S. A. Teukolsky, W. T. Vetterling, and B. P. Flannery, *Numerical Recipes in C: The Art of Scientific Computing*, Cambridge University Press, Cambridge, 1992.